Arabian Journal of Chemistry (2014) 7, 781–787

King Saud University

Arabian Journal of Chemistry

www.ksu.edu.sa
www.sciencedirect.com

ORIGINAL ARTICLE

New dicationic piperidinium hexafluorophosphate ILs, synthesis, characterization and dielectric measurements

Boumediene Haddad [a,b], Didier Villemin [b,*], El-habib Belarbi [a], Nathalie Bar [b], Mustapha Rahmouni [a]

[a] *Department of Chemistry, Synthesis and Catalysis Laboratory LSCT, Tiaret University, Tiaret, Algeria*
[b] *LCMT, ENSICAEN, UMR 6507 CNRS, University of Caen, 6 bd Ml Juin, 14050 Caen, France*

Received 11 November 2010; accepted 4 January 2011
Available online 8 January 2011

KEYWORDS

Ionic liquids;
Bis-piperidinium;
Hexafluorophosphate anion;
Dielectric relaxation;
Conductivity

Abstract A new class of dicationic ionic liquids (ILs) were synthesized for electrochemical applications at high temperatures. The syntheses are based on a dialkylation reaction of N-alkylpiperidine followed by anion exchange. The structures of ILs, based on piperidinium combined with hexafluorophosphate anion, were identified by using ^{1}H, ^{13}C, ^{19}F, ^{31}P NMR and FT-IR spectroscopy. ILs' thermal properties were investigated in the temperature range from −50 to 350 °C by using differential scanning calorimetry (DSC). In the frequency of 10^{-2}–10^{6} Hz range, dielectric measurements were performed on ILs' samples at various temperatures from −80 to 20 °C, i.e. around the glass transition temperature. The peak relaxation was observed near to this temperature. Also, the conductivity was investigated and the energy activation determined. The temperature dependence of the relaxation times was shown to be governed by the Arrhenius equation.

1. Introduction

Ionic liquids (ILs) are salts with an organic cation and an anion, which can be either organic or inorganic. Most of the cations are derived from either the imidazolium or pyridinium rings (Min et al., 2007), but phosphonium and ammonium-derivated cations can be also used in the synthesis (Ramnial et al., 2005; Gerritsma et al., 2004). Many different types of anions are used together with the mentioned cations: halides, borates, phosphates, sulfates, sulfonates, imides, etc. This provides several possibilities for both ILs syntheses and applications. The physical and chemical properties can be tailored by using different ions and also by either alkylating or functionalizing existing ions, which provide the task-specific ILs.

During the last decade, ILs have been considered as promising green reaction media and as novel solvents (Rogers and Voth, 2007; Wasserscheid and Welton, 2003; Wilkes, 2002;

* Corresponding author. Tel.: +33 213 45 28 40; fax: +33 231 45 28 77.
E-mail address: didier.villemin@ensicaen.fr (D. Villemin).
Peer review under responsibility of King Saud University.

ELSEVIER Production and hosting by Elsevier

http://dx.doi.org/10.1016/j.arabjc.2011.01.002
1878-5352 © 2011 Production and hosting by Elsevier B.V. on behalf of King Saud University.

Rogers and Seddon, 2002). Initially, ILs were developed by electrochemists (Ohno, 2005; Appetecchi et al., 2009; MacFarlane et al., 2007; Galinski et al., 2006), who were looking for ideal electrolytes suitable for batteries (Sun and Dai, 2010; Balakrishnan et al., 2006; Wu et al., 2010; Matsumoto et al., 2005). Owing to the ionic environment effect on the chemical reactions (Haumann and Riisager, 2008; Olivier-Bourbigou and Magna, 2002; Martins et al., 2008; Fraga-Dubreuil et al., 2002), the main focus of electrochemists was shifted to general ionic liquid characterization in view to better applications. Ionic liquids currently have a large variety of application field, which continue to expand because of their use as electrolytes for devices and processes, and solvents for organic/catalytic processes and separation/extraction (Han and Armstrong, 2007; Visser et al., 2002; Huddleston et al., 1998). In addition, other applications in enzyme catalysis and multiphase bio-process operations were reported (Liu and Xiao, 2007).

Many papers reported on the physicochemical properties of ILs piperidinium (Yim et al., 2007; Sakaebe and Matsumoto, 2003; Lewandowski and Olejniczak, 2007; Profatilova et al., 2009; Salminen et al., 2007; Bazito et al., 2007), but they revealed, however, that the toxicity of ILs pyridinium and piperidinium proportionately increases with the alkyl chain length. The dicationic ILs contain two head groups and two aliphatic chains linked by either a rigid or a flexible spacer (Ito et al., 2000). Besides the cation–anion combination, simple changes in the length of the spacer or in the aliphatic chains of the cations allow to modify ILs' physical properties.

In this work, novel ionic liquids (ILs) based on piperidinium hexafluorophosphate as bis-methyl piperidinium butylidene [MBPPI$^+$], bis-methyl piperidinium propylidene [MPrPPI$^+$] and bis-ethyl piperidinium butylidene [EBPPI$^+$] cations were prepared and characterized. The structures of these compounds were identified by using ^{1}H, ^{13}C, ^{19}F, ^{31}P NMR and FT-IR spectroscopy. The phase behavior change for each ILs was measured in the temperature range from −50 to 350 °C. The temperature and frequency dependences of the loss tangent (tan δ), dielectric constant (ε', ε'') and conductivity were investigated.

2. Experimental

2.1. Reagents and materials

The reagents used in this study are: 1,3-dibromopropane (98 wt.%), 1,4-dibromobutane (99.5 wt.%), *N*-methyl piperidine (95 wt.%), *N*-ethyl piperidine (97 wt.%), ammonium hexafluorophosphate (99.5 wt.%), diethyl ether and *N*,*N*-dimethylformamide. They were purchased from Fluka and used as received. Deionized H_2O was obtained by using a Millipore ion-exchange resin deionizer.

2.2. Synthesis and characterization

The general synthesis of the studied ionic liquids is illustrated in Scheme 1. The syntheses are based on the anion exchange from bromide to hexafluorophosphate. The reaction conditions of dicationic substituted piperidiniums and the obtained yields are summarized in Table 1. The synthesis of bis-methyl piperidinium butylidene bromide is taken as an example for experimental descriptions.

2.2.1. NMR and infrared spectroscopy measurements

^{1}H NMR (400 MHz), ^{13}C NMR, ^{31}P, ^{19}F (100.6 MHz) spectra were recorded on DRX 400 MHz spectrometer. The chemical shifts (δ) are given in ppm and referenced to the internal solvent signal, namely TMS, H_3PO_4 and $CFCl_3$, respectively. IR spectra were recorded on an FT-IR Perkin–Elmer Spectrum BX spectrophotometer with a resolution of 4 cm^{-1} in the range of 4000–650 cm^{-1}.

Table 1 Reaction conditions used for the synthesis of dicationic piperidinium bromides.

ILs	Alkyl side chain	Time (h)	Yield (%)
$[(CH_3\ PPI^+)_2(CH_2)_4]$	$Br(CH_2)_4Br$	6	73
$[(CH_3\ PPI^+)_2(CH_2)_3]$	$Br(CH_2)_3Br$	4	81
$[(C_2H_5\ PPI^+)_2(CH_2)_4]$	$Br(CH_2)_4Br$	7	74

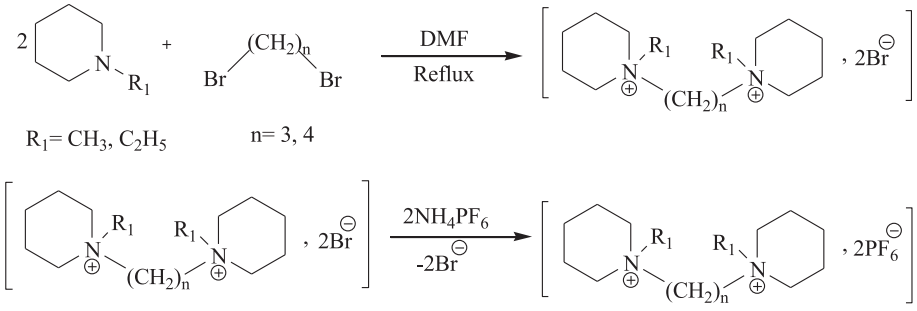

Scheme 1 General synthesis of dicationic piperidinium ionic liquids.

2.2.2. Synthesis of bis-methyl piperidinium butylidene bromide [$MBPPI^+$][$2Br^-$]

The synthesis procedure was carried out as reported elsewhere (Ito et al., 2000; Nakajima and Ohno, 2005). Briefly, *N*-methyl piperidine (12.15 mL, 100 mmol) and 1,4-dibromobutane (5.21 mL, 50 mmol) were dissolved in DMF (20 mL) before being stirred at 70 °C for 6 h. The obtained mixture was evaporated under vacuum and washed then with diethyl ether (100 mL) to give the bis-methyl piperidinium butylidene bromide as a yellowish solid (13.20 g, 31.86 mmol).

2.2.3. Synthesis of bis-methyl piperidinium butylidene hexafluorophosphate [$MBPPI^+$][PF_6^-]

Ammonium hexafluorophosphate (1.63 g, 10 mmol) dissolved in 15 mL of deionized water was added in a flask containing [$MBPPI^+$][$2Br^-$] (2.07 g, 5 mmol) dissolved in 15 mL of deionized water. The mixture consisted of two separate phases: ionic liquid at the bottom and aqueous solution at the top. The former was separated from the latter by centrifugation (3000 rpm) for 60 s. After isolation, the ionic liquid was dried in a phosphorus pentoxide P_2O_5 to remove residual water. The obtained product is a white solid (4.96 g, 12.42 mmol). The spectra details are given below:

^{1}H NMR (DMSO-d_6) δ ppm: 1.62 (m, 4H, $2\times CH_2CH_2$-CH_2), 2.57 (m, 12H, $6\times CH_2CH_2CH_2$), 2.92 (t, 12H, $6\times CH_2$-CH_2N), 3.40 (s, 6H, $2\times NCH_3$); ^{13}C NMR (DMSO-d_6) δ ppm: 20.41, 31.69, 34.98, 36.77, 61.53; ^{31}P NMR (DMSO-d_6) δ ppm: −144.20 (septet, PF_6^-); ^{19}F NMR (DMSO-d_6) δ ppm: −70.95, −72.85 (d, PF_6^-). IR: 2950 [ν(C–H)], 1467[δ(C–H)], 1279 [ν(C–N)], 814 [ν(P–F)].

2.2.4. Synthesis of bis-methyl piperidinium propylidene hexafluorophosphate [$MPrPPI^+$][PF_6^-]

Following the similar procedure, [$MPrPPI^+$][PF_6^-] was obtained as a slightly yellowish solid (6.60 g, 17.12 mmol) with the yield of 63%.

^{1}H NMR (D_2O) δ ppm: 1.63 (m, 4H, $2\times CH_2CH_2CH_2$), 1.85 (m, 8H, $4\times CH_2CH_2CH_2$), 2.29 (m, 2H, $CH_2CH_2CH_2$), 3.05 (s, 6H, $2\times NCH_3$), 3.34–3.36 (t, 12H, $6\times NCH_2CH_2$); ^{13}C NMR (D_2O) δ ppm: 15.13, 19.51, 20.40, 47.70, 59.63, 61.63; ^{31}P NMR (D_2O) δ ppm: −144.21 (septet, PF_6^-); ^{19}F NMR (D_2O) δ ppm: −69.17, −71.06 (d, PF_6^-). IR: 2956 [ν(C–H)], 1466 [δ(C–H)], 1227 [ν(C–N)], 827 [ν(P–F)].

2.2.5. Synthesis of bis-ethyl piperidinium butylidene hexafluorophosphate [$EBPPI^+$][PF_6^-]

The procedure previously described for [$MBPPI^+$][PF_6^-] was followed. A yellow solid was obtained (3.48 g, 8.14 mmol) with the yield of 66%.

^{1}H NMR (DMSO-d_6) δ ppm: 1.23–1.19 (t, 6H, J = 7.2 Hz, $2\times NCH_2CH_3$), 1.58–1.55 (q, 4H, J = 6 Hz, $2\times CH_2CH_2$-CH_2), 1.81–1.77 (q, 12H, J = 4.8 Hz, $6\times CH_2CH_2CH_2$), 2.51–2.49 (m, 12H, J = 1.6 Hz, $6\times CH_2CH_2N$), 3.39–3.34 (m, 4H, J = 6.8 Hz, NCH_2CH_3); ^{13}C NMR (DMSO-d_6) δ ppm: 8.12, 20.02, 21.17, 31.57, 36.63, 58.94; ^{31}P NMR (DMSO-d_6) δ ppm: −139.81 (septet, PF_6^-); ^{19}F NMR (DMSO-d_6) δ ppm: −71.43, −73.32 (d, PF_6^-). IR: 2951 [ν(C–H)], 1463 [δ(C–H)], 1281 [ν(C-N)], 825 [ν(P-F)].

2.3. Thermal analysis

Differential scanning calorimetry (DSC) thermograms were recorded by using a NETZSCH DSC 204 F1 instrument. The sample (3–9 mg) was placed in an aluminum pan and cooled from room temperature to −50 °C for 3 min. Subsequently, a heating scan was performed from −50 to 350 °C at a heating rate of 10 °C.min^{-1}. The DSC study on ILs shows endothermic peaks at temperatures below 140 °C for the first heating scan. The melting point was determined from the peak onset on heating. No phase transition was detected on cooling scan in the studied temperature range.

2.4. Measurement of dielectric properties

The dielectric measurements were performed on pellets processed by applying uniaxial pressure on powder. Dielectric spectra were recorded by using BDS-4000 Novocontrol spectrometer, which was coupled with the quarto system to ensure the temperature variation from −80 to 20 °C for the frequency range (10^{-2} to 10^6 Hz). For conductivity data analysis, the complex conductivity is defined as:

$$\sigma^* = \sigma' + i\sigma'' \quad (1)$$

where (σ') and (σ'') are calculated from the complex permittivity as illustrated from the Eqs. (2) and (3), respectively.

$$\sigma' = \varepsilon_0\omega\varepsilon'' \quad (2)$$

$$\sigma'' = \varepsilon_0\omega\varepsilon' \quad (3)$$

where ε_0 and ω refer to the permittivity of free space and angular frequency ($\omega = 2\pi f$), respectively.

3. Results and discussion

3.1. Infrared spectroscopy

The obtained characteristic IR bands of ILs showed that the strong peak centered at 2950–2956 cm^{-1} can be attributed to C–H stretching vibrations in the alkyl chains of the cation, as reported by Zaitsau et al. (Young Kim et al., 2008; Shi and Deng, 2005; Perchard and Novak, 1967; Zaitsau et al., 2006). Another strong peak is observed in the range of 1463–1467 cm^{-}1, which is readily assigned to the CH_3 bending vibrations (Chowdhury and Thynell, 2006; Nanbu et al., 2003). The C–N stretching vibrations of the piperidinium ring are evidenced in the 1227–1281 cm^{-1} regions. The [PF_6^-] anion exhibits a peak at 814–827 cm^{-1}, which was observed at 857 cm^{-1} in the [$BMIM^+$][PF6$^-$] and at 808 cm^{-1} in geminal imidazolium by Wagner et al. (2010) and Ding et al. (2007), respectively. Nevertheless, it should be noticed that some bands were located at 1656 and 3640 cm^{-1}, indicative of the water traces present in [$MBPPI^+$][PF6$^-$].

3.2. Thermal properties

ILs thermal behavior was investigated by using DSC method. The melting point, T_m, solid–solid transition, T_{s-s}, glass transition, T_g, decomposition, T_d, and enthalpy of melting, ΔH_m, temperatures were determined and summarized in Table 2.

Table 2 Thermal properties of dicationic piperidinium ionic liquids.

ILs	MW[a] (g mol^{-1})	T_g[b] (°C)	T_{s-s}[c] (°C)	T_m[d] (°C)	ΔH_m[e] (J.g^{-1})	T_d[f](°C)
[MBPPI$^+$][PF$_6^-$]	399.24	–	–	103.36	15.29	336.00
[MPrPPI$^+$][PF$_6^-$]	385.39	21.42	–	137.00	22.27	303.73
[EBPPI$^+$][PF$_6^-$]	427.47	−1.80	74.30	123.15	14.26	283.00

– = Not detected.
[a] Molecular weight.
[b] Glass transition temperature (T_g).
[c] Solid–solid transition temperature (onset of solid–solid peak) (T_{s-s}).
[d] Melting point (onset of the endothermic peak) (T_m).
[e] Enthalpy of melting temperature.
[f] Decomposition temperature (position of decomposition peak) (T_d).

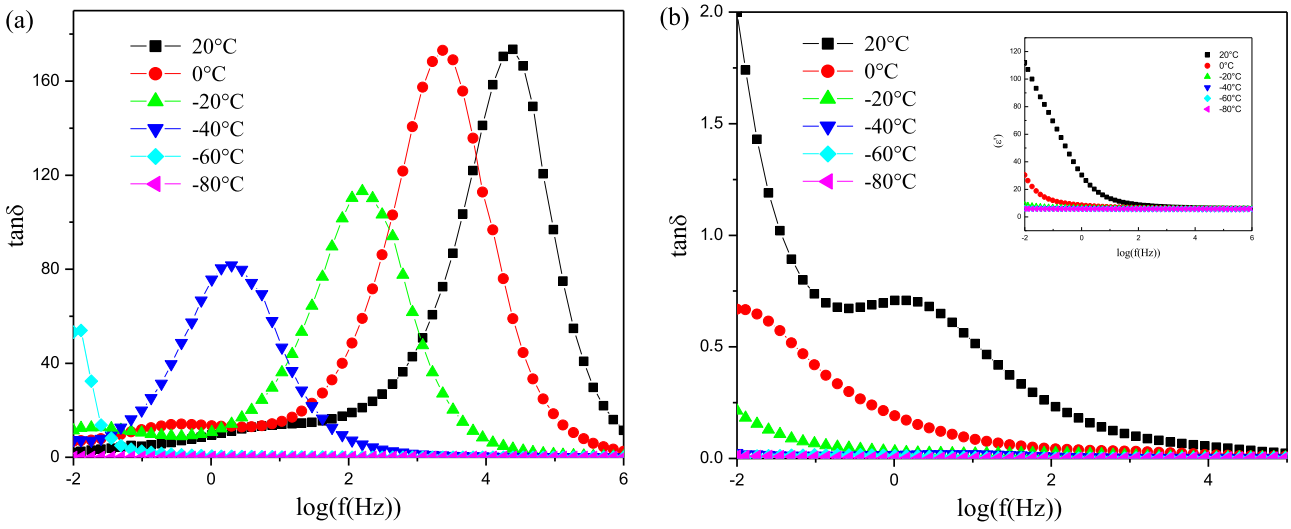

Figure 1 Frequency dependence of the loss factor tan δ measured at different temperatures of (a) [MBPPI$^+$][PF$_6^-$] and (b) [MPrPPI$^+$][PF$_6^-$].

For both [EBPPI$^+$][PF$_6^-$] and [MPrPPI$^+$][PF$_6^-$], the glass transition was observed on heating scan by small peaks at −1.80 and 21.42 °C, respectively, as result of a change from thermograms baseline. Nevertheless, [MBPPI$^+$][PF$_6^-$] did not exhibit this transition behavior under the same experimental conditions. In the case of the [EBPPI$^+$][PF$_6^-$], only one solid–solid transition at 74.2 °C was observed before melting point.

The melting points for [MBPPI$^+$], [MPrPPI$^+$] and [EBPPI$^+$] hexafluorophosphate are visibly recoded at 103.3, 137.9 and 123.1 °C, respectively (onset of the endothermic peak). For all synthesized ILs, the melting points were slightly higher than 100 °C, which can be suitable for solid electrolyte applications (Heintz et al., 2002; Fuller et al., 1998). A few weak peaks observed on the DSC curve of the [EBPPI$^+$][PF$_6^-$] and [MBPPI$^+$][PF$_6^-$] can probably be originated from minor impurity in ILs. On other hand, the cations symmetry of our ILs has a remarkable role in the increase of the melting transition point.

The studied ILs exhibit different decomposition temperature values which are included in 280–340 °C range (Table 2). Such result is not probably relevant from the difference in the chain lengths of cations.

3.3. Dielectric analysis

The complex permittivity can be expressed as a complex number:

$$\varepsilon^*(\omega) = \varepsilon' - i\varepsilon'' \tag{4}$$

The real part $\varepsilon'(\omega)$ and imaginary one $\varepsilon''(\omega)$ of the complex permittivity spectra are determined. Consequently, the loss factor is calculated as follows:

$$\tan(\delta(\omega)) = \frac{\varepsilon''(\omega)}{\varepsilon'(\omega)} \tag{5}$$

With respect to the different temperatures, the relaxation time, τ, is calculated according to the resonance condition, which is defined by $\omega\tau = 1$ from the peak maximum of $\tan(\delta(\omega))$ as shown in Fig. 1(a) and (b).

These figures show the dielectric spectra in terms of the loss factor $\tan\delta = \varepsilon''/\varepsilon'$ versus the frequency for two ILs [MBPPI$^+$] and [MPrPPI$^+$] hexafluorophosphate. For [MBPPI$^+$][PF$_6^-$], the maximum in the tan δ peak shifts to higher frequency with temperature elevation. We noticed clearly that larger tan δ values are for higher temperatures.

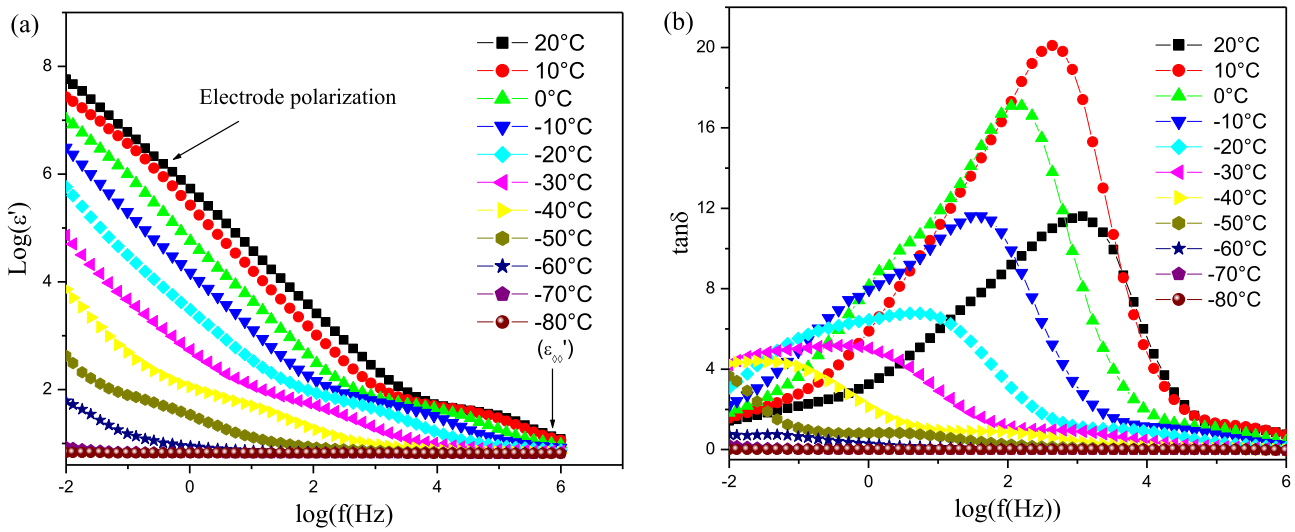

Figure 2 Frequency dependence of (a) ε' and (b) tan δ at the different temperatures for [EBPPI$^+$][PF$_6^-$].

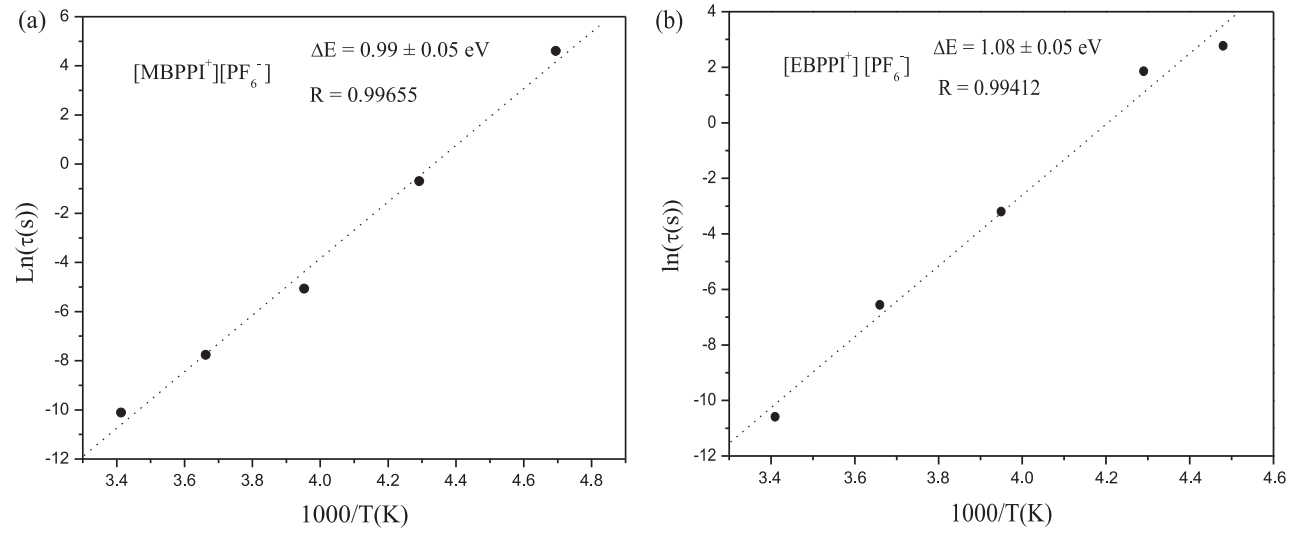

Figure 3 Temperature dependence of the relaxation times: Arrhenius plot of logarithm ln τ (●) vs. reciprocal of temperature $1/T$. (·····) Linear regression line. (R) correlation coefficient.

Moreover, the relaxation peak is observed for the sample [MPrPPI$^+$][PF$_6^-$] subjected to a temperature near T_g, i.e. roughly 20 °C (Fig. 1(b)). Near this temperature, the mobility of the ions is quite high, the result is that the polarisability suddenly increases at T_g resulting in a peak on tan δ as frequency; previous studies (Adachi and Hirano, 1998; Goitiandia and Alegría, 2004; Pradhan and Iannacchione, 2010) showed that the dielectric T_g originates from the reorientation of molecules.

The real permittivity part ε' and the loss factor tan δ versus the frequency for different temperatures are given in Fig. 2. For [EBPPI$^+$][PF$_6^-$] (Fig. 2 (a)), we observe that the dielectric permittivity, ε', reduces with the temperature and the frequency increasing, converging to a constant value, ε'_∞, whatever applied temperature. This result is probably indicative of rapid polarization processes.

On the other hand, the large values of the permittivity ε', obtained in the low frequency range, is attributed to the electrode polarization phenomenon occurring as a result of ions accumulation near the electrodes (Furukawa et al., 1997).

The relaxation phenomenon occurs near to T_g in [EBPPI$^+$][PF$_6^-$], which confirms the result obtained for [MPrPPI$^+$][PF$_6^-$] (Fig. 1(b)), Near T_g.

3.3.1. Conductivity

In order to understand the ion dynamics in ILs, the conductivity of our samples was determined at different temperatures. Generally, the conductivity increases as the temperature is elevated. The sample [EBPPI$^+$][PF$_6^-$] exhibits conductivity values larger than those of [MPrPPI$^+$][PF$_6^-$] but lower compared with [MBPPI$^+$][PF$_6^-$]. In fact, for a temperature of 20 °C, the con-

ductivity of [EBPPI$^+$][PF_6^-] is 2.6×10^2 times larger than that of [MPrPPI$^+$][PF_6^-], but about 44 times lower than that of [MBPPI$^+$][PF_6^-].

The activation barrier, ΔE, is calculated from the mean relaxation time, τ, based on the formula,

$$\tau = \tau_0 \exp\left[\frac{\Delta E}{K_B T}\right] \quad (6)$$

where ΔE, τ_0 and K_B are the activation energy, the pre-exponential factor and the Boltzmann constant, respectively.

The linear relationship between ln τ and $1/T$ is evidenced in Fig. 3. The activation energies are 0.99 ± 0.05 and 1.08 ± 0.05 eV for [MBPPI$^+$][PF_6^-] and [EBPPI$^+$][PF_6^-], respectively. The obtained values are comparable, which can be related to the similar length chain of two ILs. Unfortunately, the range of temperature was not enough to determine the activation energy of [MPrPPI$^+$][PF_6^-].

4. Conclusion

Novel ionic liquids (ILs) based on the piperidinium hexafluorophosphate as bis-methyl piperidinium butylidene [MBPPI$^+$], bis-methyl piperidinium propylidene [MPrPPI$^+$] and bis-ethyl piperidinium butylidene cations were successfully synthesized. The thermal investigations have revealed that the melting points were slightly higher than 100 °C, which may be of interest for solid electrolyte applications. The relaxation peak is observed for [MPrPPI$^+$] and [EBPPI$^+$] hexafluorophosphate near to glass transition temperature, T_g. For the latter sample, the large values of the permittivity, ε', obtained in the low frequency range, are attributed to the electrode polarization phenomenon occurring as a result of an ions accumulation near the electrodes. The conductivity increased with the applied temperature. At 20 °C, the conductivity of [EBPPI$^+$][PF_6^-] is 2.6×10^2 times larger than that of [MPrPPI$^+$][PF_6^-], but about 44 times lower than that of [MBPPI$^+$][PF_6^-]. The activation energies of [MBPPI$^+$][PF_6^-] and [EBPPI$^+$][PF_6^-] are found to be (0.99 ± 0.05) and (1.08 ± 0.05) eV, for conduction process.

Acknowledgements

We gratefully acknowledge the program national exceptional (PNE-Algeria) for its financial support. The authors thank the Head of the CMOS laboratory, Montpellier University and his group for Differential Scanning Calorimetry (DSC). We are thankful to the PMDP team from Charles Gherardt Institute, Montpellier II University for his assistance in the dielectric measurements of the ionic liquids.

References

Adachi, K., Hirano, H., 1998. Macromolecules 31, 3958–3962.
Appetecchi, G.B., Montanino, M., Zane, D., Carewska, M., Alessandrini, F., Passerini, S., 2009. Electrochim. Acta 54, 1325–1332.
Balakrishnan, P.G., Ramesh, R., Prem Kumar, T., 2006. J. Power Sources 155, 401–414.
Bazito, F.C., Kawano, Y., Torresi, R.M., 2007. Electrochim. Acta 52, 6427–6437.
Chowdhury, A., Thynell, S.T., 2006. Thermochim. Acta 443, 159–172.
Ding, Y.-S., Zha, M., Zhang, J., Wang, S.-S., 2007. Chin. Chem. Lett. 18, 48–50.
Fraga-Dubreuil, J., Bourahla, K., Rahmouni, M., Bazureau, J.P., Hamelim, J., 2002. J. Catal. Commun. 3, 185–190.
Fuller, J., Breda, A.C., Carlin, R.T., 1998. J. Electroanal. Chem. 459, 29–34.
Furukawa, T., Imura, M., Yuruzume, H., 1997. Jpn. J. Appl. Phys. 36, 1119–1125.
Galinski, M., Lewandowski, A., Stepniak, I., 2006. Electrochim. Acta 51, 5567–5580.
Gerritsma, D.A., Robertson, A., McNulty, J., Capretta, A., 2004. Tetrahedron Lett. 45, 7629–7631.
Goitiandia, L., Alegría, A., 2004. J. Chem. Phys. 121, 1636–1643.
Han, X., Armstrong, D.W., 2007. Acc. Chem. Res. 40, 1079–1086.
Haumann, M., Riisager, A., 2008. Chem. Rev. 108, 1474–1497.
Heintz, A., Kulikov, D.V., Verevkin, S.P., 2002. J. Chem. Thermodyn. 34, 1341–1347.
Huddleston, J.G., Willauer, H.D., Swatloski, R.P., Visser, A.E., Rogers, R.D., 1998. Chem. Commun., 1765–1766.
Ito, K., Nishina, N., Ohno, H., 2000. Electrochim. Acta 45, 1295–1298.
Lewandowski, A., Olejniczak, A., 2007. J. Power Sources 172, 487–492.
Liu, S., Xiao, J., 2007. J. Mol. Catal. A: Chem. 270, 1–43.
MacFarlane, D.R., Forsyth, M., Howlett, P.C., Pringle, J.M., Sun, J., Annat, G., Neil, W., Izgorodina, E.I., 2007. Acc. Chem. Res. 40, 1165–1173.
Martins, M.A.P., Frizzo, C.P., Moreira, D.N., Zanatta, N., Bonacorso, H.G., 2008. Chem. Rev. 108, 2015–2050.
Matsumoto, H., Sakaebe, H., Tatsumi, K., 2005. J. Power Sources 146, 45–50.
Min, G.-H., Yim, T., Lee, H.Y., Kim, H.-J., Mun, J., Kim, S., Oh, S.M., Kim, Y.G., 2007. Bull. Korean Chem. Soc. 28, 1562–1566.
Nakajima, H., Ohno, H., 2005. Polymer 46, 11499–11504.
Nanbu, N., Sasaki, Y., Kitamura, F., 2003. Electrochem. Commun. 5, 383–387.
Ohno, H. (Ed.), 2005. Electrochemical Aspects of Ionic Liquids. Wiley-Interscience, Hoboken, New Jersey (Chapter 4).
Olivier-Bourbigou, H., Magna, L., 2002. J. Mol. Catal. A: Chem. 182, 419–437.
Perchard, C., Novak, A., 1967. Spectrochim. Acta Part A 23, 1953–1968.
Pradhan, N.R., Iannacchione, G.S., 2010. J. Appl. Phys. 43, 1–7.
Profatilova, I.A., Choi, N.S., Roh, S.W., Kim, S.S., 2009. J. Power Sources 192, 636–643.
Ramnial, T., Daisuke, D.I., Clyburne, J.A.C., 2005. Chem. Commun., 325–327.
Rogers, R.D., Seddon, K.R. (Eds.), 2002. Â Ionic Liquids: Industrial Applications to Green Chemistry, Â ACS Symposium Series, vol. 818, American Chemical Society, Washington, DC.
Rogers, R.D., Voth, G.A., 2007. Acc. Chem. Res. 40, 1077–1078.
Sakaebe, H., Matsumoto, H., 2003. Electrochem. Commun. 5, 594–598.
Salminen, J., Papaiconomou, N., Kumar, R.A., Lee, J.M., Kerr, J., Newman, J., Prausnitz, J.M., 2007. Fluid Phase Equilib. 261, 421–426.
Shi, F., Deng, Y., 2005. Spectrochim. Acta Part A 62, 239–244.
Sun, X.G., Dai, S., 2010. Electrochim. Acta 55, 4618–4626.
Visser, A.E., Swatloski, R.P., Reichert, W.M., Mayton, R., Sheff, S., Wierzbicki, A., Davis, J.H., Rogers, R.D., 2002. Environ. Sci. Technol. 36, 2523–2529.
Wagner, M., Kvarnström, C., Ivaska, A., 2010. Electrochim. Acta 55, 2527–2535.
Wasserscheid, P., Welton, T., 2003. Ionic Liquids in Synthesis, Second ed. Wiley-VCH, Verlag, Weinheim.

Wilkes, J.S., 2002. Green Chem. 4, 73–80.
Wu, T.Y., Su, S.G., Gung, S.T., Lin, M.W., Lin, Y.C., Lai, C.A., Sun, I.W., 2010. Electrochim. Acta 55, 4475–4482.
Yim, T., Lee, H.Y., Kim, H.-J., Mun, J., Kim, S., Oh, S.M., Kim, Y.G., 2007. Bull. Korean Chem. Soc. 28, 1567–1572.
Young Kim, J., Ho Kim, T., Young Kim, D., Park, N.G., Ahn, K.D., 2008. J. Power Sources 175, 692–697.
Zaitsau, D.H., Kabo, G.J., Strechan, A.A., Paulechka, Y.U., Tschersich, A., Verevkin, S.P., Heintz, A., 2006. J. Phys. Chem. A 10, 7303–7306.